ROYAL SOCIETY
OF CHEMISTRY

COMMUNICATION

CrossMark
click for updates

Label-free nanoprobe for antibody detection through an antibody catalysed water oxidation pathway†

Kyeonghye Guk,[ac] Hyeran Kim,[b] Yujeong Kim,[ac] Taejoon Kang,[abc] Eun-Kyung Lim[*abc] and Juyeon Jung[*ac]

We developed a nanoprobe for the label-free detection of antibodies associated with infectious diseases, through a method based on the antibody catalyzed water oxidation pathway (ACWOP). First, methoxy poly(ethylene glycol) (mPEG)–chlorin e6 was chemically conjugated to mPEG and chlorin e6 by esterification, to enable both singlet oxygen generation and loading of coumarin boronate. Subsequently, the nanoprecipitation method was used for spontaneous nanoprobe self-assembly from coumarin boronate and mPEG–chlorin e6, which resulted in a mean nanoprobe size of ∼200 nm. The potential of the nanoprobe as an antibody detection agent was evaluated by using human immunoglobulin antibodies as a model antibody. We confirmed that the nanoprobe generated singlet oxygen ($^1O_2$) via the photodynamic chemical effect of the chlorin e6 in mPEG–chlorin e6 and that water (H_2O) was subsequently oxidized to hydrogen peroxide (H_2O_2) in the presence of the singlet oxygen through the ACWOP. The generated H_2O_2 was detected via the fluorescence of coumarin boronate in the nanoprobe. Specifically, the fluorescence intensity increased linearly with increasing antibody amounts, thus demonstrating the potential of the system as an alternative method for label-free antibody detection.

The enzyme-linked immunosorbent assay (ELISA) was developed in 1971 by Engall and Perlmann and by van Weemen and Schuurs.[1,2] Since then, ELISA has been widely used to detect polyclonal and monoclonal antibodies associated with infectious disease in biological fluids and culture media.[3,4] This technique has been widely used to detect antigen-specific

[a]Hazards Monitoring BioNano Research Center, Korea Research Institute of Bioscience and Biotechnology, Daejeon 34141, Republic of Korea. E-mail: eklim1112@kribb.re.kr; jjung@kribb.re.kr; Tel: +82-42-879-8456

[b]BioNano Health Guard Research Center, Korea Research Institute of Bioscience and Biotechnology (KRIBB), Daejeon 34141, Republic of Korea

[c]Major of Nanobiotechnology and Bioinformatics, University of Science and Technology, Daejeon 34113, Republic of Korea

† Electronic supplementary information (ESI) available: Experimental details; preparation and characterization of mPEG–chlorin e6 and nanoprobe, measurement of IgG antibody using nanoprobe. See DOI: 10.1039/c6ra16911b
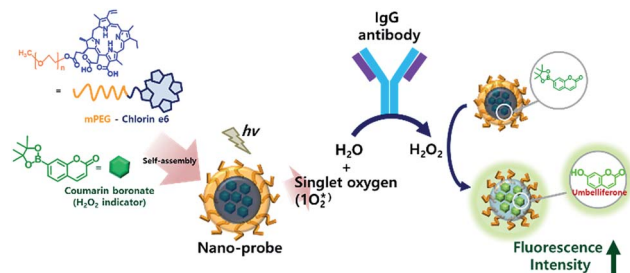
antibodies after vaccination or antibodies for the diagnosis of infectious diseases, although ELISA is not a generally accepted methodology for such purposes because of a lack of uniform standards.[5–12] ELISA is the most widely used method for accurate, convenient, and robust detection based on antibody-antigen specific binding and is performed in 4 steps: (i) immobilization of the capture antibody on a microplate, (ii) incubation with an antigen-containing sample, (iii) binding of the antigen to the capture antibody, and (iv) addition of an enzyme (*e.g.*, horseradish peroxidase (HRP), alkaline phosphatase, or β-galactosidase)-conjugated secondary antibody to generate a measurable signal.[12] Among enzymes, HRP is widely used because it is smaller, more stable, and less expensive than other enzymes. However, the secondary antibody used in this step is strongly dependent on the specificity, class and species of the antibody. Both the analytical time and the risk of nonspecific binding are increased by the use of secondary reagents, which may lead to false positives.[2,11] Wentworth *et al.* have demonstrated that most antibodies can convert molecular oxygen to hydrogen peroxide (H_2O_2) in a catalytic process in which water (H_2O) is oxidized to H_2O_2 by singlet oxygen molecules ($^1O_2$).[13–16] Nieva *et al.* have described the singlet oxygen reaction with H_2O, which produces H_2O_2 in a process termed the antibody-catalyzed water oxidation pathway (ACWOP).[13–19] Additionally, Wentworth *et al.* have demonstrated that the ACWOP occurs independently of the specificity, class, and species of antibody. Many researchers have reported that antibodies perform a catalytic role in the conversion of singlet oxygen plus water to H_2O_2.[13,18] Recently, H_2O_2 generated with an antibody has been successfully detected by using electrochemical methods, as confirmed by Elizabeth Welch *et al.* in 2014.[19] Nano-sized materials have several advantages of measuring enzyme activity with high accuracy and precision because of unique properties. Its higher surface areas facilitate faster response and improved catalytic activities.[20–22] In this report, we describe a label-free detection system for immunoglobulin antibodies, using a nanoprobe that detects by ACWOP without a need for secondary reagents. For the fabrication of the

Fig. 1 Schematic illustration of the label-free antibody detection process using the nanoprobe.

Fig. 2 (a) Morphologies of the nanoprobe, as determined by SEM and (b) the absorbance spectrum.

nanoprobe, methoxy poly(ethylene glycol) (mPEG)–chlorin e6 was first synthesized from mPEG and chlorin e6 because both amphiphilic polymers are photosensitizers.[23–26] Next, coumarin boronate was combined with mPEG–chlorin e6 *via* a nanoprecipitation method to form the nanoprobe. This system proceeded in three steps (Fig. 1): (1) singlet oxygen was generated by the mPEG–chlorin e6 of the nanoprobe after UV light irradiation,[27–29] (2) the antibody produced H_2O_2 from water in the presence of singlet oxygen, and (3) the coumarin boronate in the nanoprobe was oxidized by H_2O_2 to umbelliferone,[30,31] which fluoresces.

Results and discussion

First, we synthesized mPEG–chlorin e6 *via* an esterification reaction using DCC and DMAP as the coupling agent and catalyst, respectively.[25,26] The generation of the ester group of mPEG–chlorin e6 was confirmed by FT-IR. As illustrated in Fig. S1(a),† the C=O carbonyl stretch of the aliphatic esters appeared from 1750–1735 cm^{-1}. Furthermore, we verified synthesized mPEG–chlorin e6 by the ^{1}H-NMR spectrum with $CDCl_3$ as a solvent (Fig. S1(b)†). Chlorin e6, a photosensitizer, revealed weak solubility in the aqueous phase. However, the mPEG–chlorin e6 obtained from the mPEG modification exhibited strongly enhanced solubility in the aqueous phase because of the hydrogen bonding between water molecules and the oxygen atoms of the PEG; this solubility indicated that mPEG–chlorin e6 could act as an amphiphilic polymer.

Next, we produced a nanoprobe for label-free antibody detection using mPEG–chlorin e6. Specifically, coumarin boronate, which served as a hydrogen peroxide (H_2O_2) indicator, was dissolved in acetone (polar aprotic solvent).[30,31] The coumarin boronate was stably surrounded with mPEG–chlorin e6 *via* self-assembly, using the nanoprecipitation method. The morphology and size of the nanoprobe were examined *via* field emission-scanning electron microscopy (FE-SEM) and dynamic light scattering (DLS). As illustrated in Fig. 2(a), these nanoprobes exhibited spherical shapes, and their average diameter was ~120 nm, with a consistent size distribution (118.5 ± 4.0 nm) by measuring DLS technique. Additionally, their absorption spectra indicated absorption at 400 nm and 665 nm, corresponding to the physical properties of chlorin e6 in mPEG–chlorin e6 (Fig. 2(b)).
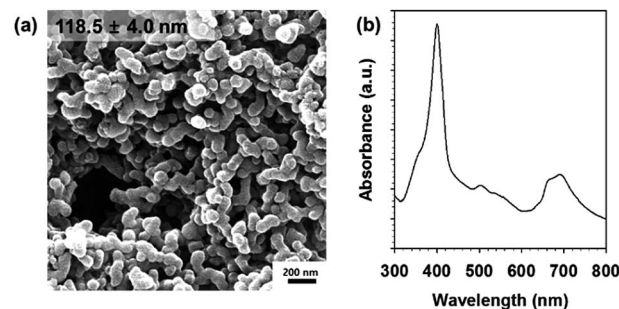
Chlorin e6 known as a photosensitizer can be illuminated in the aqueous phase, which leads to the generation of singlet oxygen ($^1O_2^*$), which is the basis of photodynamic therapy (PDT).[27–29] Using this feature, we next confirmed the singlet oxygen-generated effects of the chlorin e6-containing nanoprobe in the aqueous phase. The singlet oxygen generated by the nanoprobe was measured by using singlet oxygen sensor green reagent (SOSG) after UV irradiation at 365 nm, that SOSG reacts with the singlet oxygen and then generates SOSG-endoperoxides (SOSG-EP) by emitting strong green fluorescence. Thus, the enhancement of the fluorescence intensity indicated an increase in the singlet oxygen level. As shown in Fig. 3, the fluorescence intensities were continuously enhanced in accordance with the increased concentrations of the nanoprobe and the longer UV irradiation times. Despite the short UV irradiation time (10 min), the fluorescence intensity was enhanced by approximately 2.3-fold at 5 mM compared with the control (absence of the nanoprobe; 0 mM) because of the singlet oxygen generation. Specifically, at 1.25 mM or higher concentrations, the intensities were more than doubled regardless of time (Fig. 3(b)). These results demonstrated that the nanoprobe effectively produces singlet oxygen, which is a critical factor for antibody detection through label-free methods.

As described above, antibodies with tryptophans can catalyze the oxidation of water to H_2O_2 in the presence of singlet oxygen through the ACWOP.[13–19] First, we measured the H_2O_2 concentrations by using a commercial kit (hydrogen peroxide colorimetric detection kit) to investigate whether the singlet oxygen
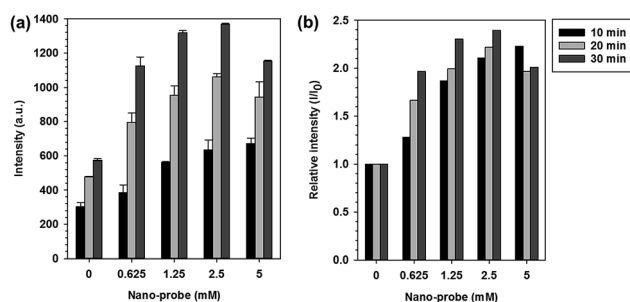

Fig. 3 Detection of singlet oxygen generation by the nanoprobe under various concentrations. (a) Fluorescence intensity of SOSG and (b) the relative intensity.
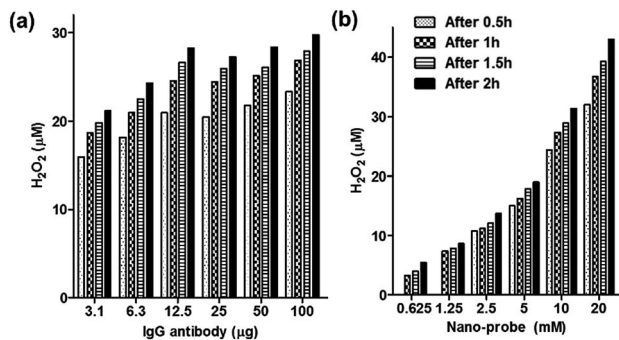
Fig. 4 Detection of hydrogen peroxide (H_2O_2) generation *via* the IgG antibody and the nanoprobe (a) with different amounts of IgG antibody and 10 mM nanoprobe and (b) with different concentrations of nanoprobe and 25 μg of IgG antibody.

Fig. 6 (a) Fluorescence intensities of the nanoprobe with different amounts of IgG antibodies. (b) Relative intensities of the nanoprobe *vs.* the IgG antibodies [relative intensity (%): (intensity − intensity$_{0\ ng}$)/ intensity$_{0\ ng}$ × 100], (red: 1 mM and blue: 2 mM).

generated by the nanoprobe could be successfully converted to H_2O_2 in the presence of the antibodies, by using different concentrations of the IgG antibodies and the nanoprobe. The IgG antibody-incubated wells treated with the nanoprobe were then exposed to UV light (λ_{ex}: 365 nm) for 10 min. After a further incubation (0.5, 1, 1.5, and 2 h), the H_2O_2 concentrations were measured. As shown in Fig. 4(a), as the antibody concentrations increased, the H_2O_2 increased. Additionally, at the same concentration of antibody (25 μg), noticeably higher amounts of H_2O_2 were produced at high nanoprobe concentrations than at low nanoprobe concentrations (Fig. 4(b)). In the presence of 20 mM nanoprobe, the H_2O_2 generation was markedly increased by approximately 8-fold relative to that at 0.625 mM, thus indicating that the production of H_2O_2 was dependent on the nanoprobe concentration in addition to the antibody concentration. These results demonstrate that the singlet oxygen generated by the nanoprobe led to H_2O_2 formation in the presence of the antibody. Next, on the basis of these results, we attempted to measure the nanoprobe measured antibody concentrations by themselves without the use of an additional kit.

After the antibody and nanoprobe incubation, this mixture was exposed under UV light for a short time (10 min), and the fluorescence intensity was then measured (λ_{ex}: 332 nm, λ_{em}: 454 nm). The coumarin boronate in the nanoprobe was oxidized by

H_2O_2 to umbelliferone, a green fluorophore with a high quantum yield.[30,31] Thus, the nanoprobe detected the produced H_2O_2 *via* both the antibody and the photosensitizer of the nanoprobe, on the basis of the emitted fluorescence.[30–34] We confirmed whether nanoprobe can be applied to various antibodies, immunoglobulin (IgG, IgM and IgE), at high concentrations (20 mM). The fluorescence intensities clearly increased as antibody concentrations increased regardless of their types. Overall intensities were enhanced by 1.5-fold more compared with that of 0 ng (control) (Fig. 5(a) and S2(a)†). Especially, although nanoprobe were in serum-containing media (1% FBS), fluorescence intensities were showed and also increased according to antibody concentrations (Fig. 5(b) and S2(b)†). This indicated that this nanoprobe activated normally in the absence or presence of serum.

Furthermore, we investigated the dependence of the fluorescence response on the antibody concentration at specific nanoprobe concentrations (1 and 2 mM), which were experimentally determined to be the optimal conditions. Although there was no substantial difference between 50 ng of antibody and 0 ng (control), the fluorescence intensity clearly increased for amounts greater than 100 ng (Fig. 6(a)). We determined the relative intensity (=intensity − intensity at 0 ng/intensity at 0 ng (%)) to estimate the possibility of the nanoprobe acting as a detection reagent at the various antibody concentrations, and we calculated the calibration curves (Fig. 6(b)). Regardless of the nanoprobe concentration, the intensity was gradually increased at higher antibody concentrations with similar linear correlations (slope = 0.124, R^2 = 0.93 at 2 mM nanoprobe and slope = 0.124, R^2 = 0.93 at 1 mM nanoprobe); thus indicating that the nanoprobe can be used to determine antibody concentration through measurement of the fluorescence intensity and comparison to the control.

Conclusions

In conclusion, we developed a new label-free IgG antibody detection method based on the ACWOP. The nanoprobe was designed as an all-in-one system for antibody detection that can autonomously generate singlet oxygen and detect the H_2O_2 produced by the ACWOP while emitting strong fluorescence.
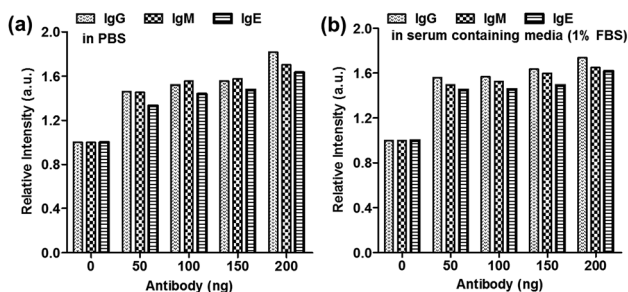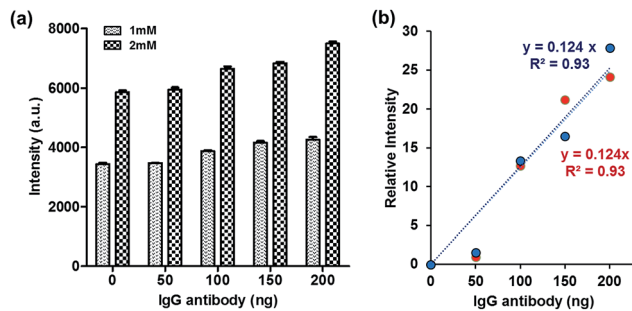

Fig. 5 The effects of the nanoprobe on the antibody detection. Relative fluorescence intensities of the nanoprobe with different amounts of various antibodies (a) in PBS and (b) in 1% FBS buffer [relative intensity: intensity/intensity$_{0\ ng}$].

We confirmed that the nanoprobe produced singlet oxygen *via* photodynamic effects and that the antibodies catalyzed the conversion of singlet oxygen plus water to hydrogen peroxide (H_2O_2). Additionally, the fluorescence of the nanoprobe was significantly increased by the generation of H_2O_2. Thus, the fluorescence intensity increased in an antibody concentration-dependent manner. On the basis of this study, we believe that this nanoprobe may potentially be applicable to detection of all antibodies, regardless of specificity. This system has tremendous potential as a simple, general method for antibody detection.

Acknowledgements

Notes and references

1 K. Miura, A. C. Orcutt, O. V. Muratova, L. H. Miller, A. Saul and C. A. Long, *Vaccine*, 2008, **26**, 193–200.
2 R. M. Lequin, *Clin. Chem.*, 2005, **51**, 2415–2418.
3 R. de la Rica and M. M. Stevens, *Nat. Protoc.*, 2013, **8**, 1759–1764.
4 J. Yamamichi, T. Ojima, K. Yurugi, M. Iida, T. Imamura, E. Ashihara, S. Kimura and T. Maekawa, *Nanomedicine*, 2011, **7**, 889–895.
5 H. Tsai, Y. H. Lu, H. X. Liao, S. W. Wu, F. Y. Yu and C. B. Fuh, *Chem. Cent. J.*, 2015, **9**, 8–14.
6 M. F. Clark and A. N. Adams, *J. Gen. Virol.*, 1977, **34**, 475–483.
7 C. K. Hsu, H. Y. Huang, W. R. Chen, W. Nishie, H. Ujiie, K. Natsuga, S. T. Fan, H. K. Wang, J. Y. Lee, W. L. Tsai, H. Shimizu and C. M. Cheng, *Anal. Chem.*, 2014, **86**, 4605–4610.
8 Q. L. Liu, X. H. Yan, X. M. Yin, B. Situ, H. K. Zhou, L. Lin, B. Li, N. Gan and L. Zheng, *Molecules*, 2013, **18**, 12675–12686.
9 M. S. Ozdemir, M. Marczak, H. Bohets, K. Bonroy, D. Roymans, L. Stuyver, K. Vanhoutte, M. Pawlak and E. Bakker, *Anal. Chem.*, 2013, **85**, 4770–4776.
10 Z. Shen, N. Hou, M. Jin, Z. Qiu, J. Wang, B. Zhang, X. Wang, J. Wang, D. Zhou and J. Li, *Gut Pathog.*, 2014, **6**, 14–21.
11 A. Voller, A. Bartlett and D. E. Bidwell, *J. Clin. Pathol.*, 1978, **31**, 507–520.
12 L. Zhan, W. B. Wu, X. X. Yang and C. Z. Huang, *New J. Chem.*, 2014, **38**, 2935–2940.
13 A. Sreedhara, K. Lau, C. Li, B. Hosken, F. Macchi, D. Zhan, A. Shen, D. Steinmann, C. Schoneich and Y. Lentz, *Mol. Pharm.*, 2013, **10**, 278–288.
14 J. Nieva and P. Wentworth Jr, *Trends Biochem. Sci.*, 2004, **29**, 274–278.
15 J. Nieva, L. Kerwin, A. D. Wentworth, R. A. Lerner and P. Wentworth Jr, *Immunol. Lett.*, 2006, **103**, 33–38.
16 A. D. Wentworth, L. H. Jones, P. Wentworth, K. D. Janda and R. A. Lerner, *Proc. Natl. Acad. Sci. U. S. A.*, 2000, **97**, 10930–10935.
17 D. Datta, N. Vaidehi, X. Xu and W. A. Goddard 3rd, *Proc. Natl. Acad. Sci. U. S. A.*, 2002, **99**, 2636–2641.
18 P. Wentworth Jr, L. H. Jones, A. D. Wentworth, X. Zhu, N. A. Larsen, I. A. Wilson, X. Xu, W. A. Goddard III, K. D. Janda, A. Eschenmoser and R. A. Lerner, *Science*, 2001, **293**, 1806–1811.
19 M. E. Welch, N. L. Ritzert, H. Chen, N. L. Smith, M. E. Tague, Y. Xu, B. A. Baird, H. D. Abruna and C. K. Ober, *J. Am. Chem. Soc.*, 2014, **136**, 1879–1883.
20 K. Ariga, J. Li, J. Fei, Q. Ji and J. P. Hill, *Adv. Mater.*, 2016, **28**, 1251–1286.
21 K. J. Cash and H. A. Clark, *Trends Mol. Med.*, 2010, **16**, 584–593.
22 N. Xia, Q. Wang and L. Liu, *Sensors*, 2015, **15**, 499–514.
23 E. K. Lim and B. H. Chung, *Nat. Protoc.*, 2016, **11**, 236–251.
24 E. K. Lim, H. O. Kim, E. Jang, J. Park, K. Lee, J. S. Suh, Y. M. Huh and S. Haam, *Biomaterials*, 2011, **32**, 7941–7950.
25 E. K. Lim, J. Yang, C. P. Dinney, J. S. Suh, Y. M. Huh and S. Haam, *Biomaterials*, 2010, **31**, 9310–9319.
26 E.-K. Lim, E. Jang, J. Kim, T. Lee, E. Kim, H. S. Park, J.-S. Suh, Y.-M. Huh and S. Haam, *J. Mater. Chem.*, 2012, **22**, 17518–17524.
27 Y. Li, Y. Yu, L. Kang and Y. Lu, *Int. J. Clin. Exp. Med.*, 2014, **7**, 4867–4876.
28 H. Park, W. Park and K. Na, *Biomaterials*, 2014, **35**, 7963–7969.
29 M. Wawrzynska, W. Kalas, D. Bialy, E. Ziolo, J. Arkowski, W. Mazurek and L. Strzadala, *Arch. Immunol. Ther. Exp.*, 2010, **58**, 67–75.
30 B. C. Dickinson, C. Huynh and C. J. Chang, *J. Am. Chem. Soc.*, 2010, **132**, 5906–5915.
31 S. Harmsen, M. A. Bedics, M. A. Wall, R. Huang, M. R. Detty and M. F. Kircher, *Nat. Commun.*, 2015, **6**, 6570–6578.
32 A. Gomes, E. Fernandes and J. L. Lima, *J. Biochem. Biophys. Methods*, 2005, **65**, 45–80.
33 M. Pázdzioch-Czochra and A. Widénska, *Anal. Chim. Acta*, 2002, **452**, 177–184.
34 L. Yuan, W. Lin, Y. Xie, B. Chen and S. Zhu, *J. Am. Chem. Soc.*, 2012, **134**, 1305–1315.